

First deep electrical resistivity structure of the southern Congo craton

David Khoza¹²³, Alan G. Jones¹, Mark R. Muller¹, Susan Webb¹², and the SAMTEX Team
¹ Dublin Institute for Advanced Studies, Dublin, Ireland
² University of the Witwatersrand, Johannesburg, South Africa
³ BHP Billiton SA, Johannesburg, South Africa

SUMMARY

The southern African tectonic fabric is made up of a number Archean cratons flanked by Proterozoic and younger mobile belts, all with distinctly different but related geological evolutions. Of these cratons the southern extent of the Congo craton is one of the least-constrained tectonic boundaries in the African tectonic architecture and knowledge of its geometry is crucial for understanding geological process of formation and deformation prevailing in the Archean and later.

In this work, which forms a component of the hugely successful Southern African MagnetoTelluric EXperiment (SAMTEX), we present the first-ever lithospheric electrical resistivity image of the southern boundary of the enigmatic Congo craton and the Neoproterozoic Damara-Ghanzi-Chobe (DGC) orogenic belt on its flanks. The DGC belt is highly complex and records the transpressive collision between the Congo to the north and Kalahari craton to the south. Magnetotelluric data were collected along a profile crossing all three of these tectonic blocks.

The two-dimensional resistivity models resulting from inverting the distortion-corrected responses along the profiles all indicate significant lateral variations in the crust and upper mantle structure along and across strike from the younger DGC orogen to the older adjacent craton. The Moho depth in the DGC is mapped at 40 km by active seismic methods, and is also well constrained by S-wave receiver function models. The Damara belt lithosphere, although generally more conductive and significantly thinner (approximately 150 km) than the adjacent Congo and Kalahari cratons, exhibits upper crustal resistive features interpreted to be caused by igneous intrusions emplaced during the Gondwanan Pan-African magmatic event. Preferential alignment of graphite along grain boundaries facilitated by deep shear movement during crustal extension and thinning could account for the high conductive region within the DGC. The Congo and Kalahari cratons are characterised by very thick and resistive lithosphere, approximately 220 km and 160 km respectively. The resistive Okavango Dyke Swam (ODS) intrudes into the DGC crust and extends to depths of approximately 70 km.

Keywords: Electrical resistivity, Archean craton, Lithosphere-Asthenosphere Boundary, Congo craton

INTRODUCTION

The cratonic margins, and some intra-cratonic domain boundaries, have played a major role in shaping the geological evolution of African lithosphere. It is thus critical to understand the sub-surface nature of these boundaries and infer their evolution.

The Damara-Ghanzi-Chobe belt (DGC) is a highly complex north-east-southwest (NE-SW) trending orogenic belt (Figure 1) recording the collision of the Kalahari craton to the south and the Congo craton to the north during the Pan-African amalgamation of Gondwana (Hanson [2003], Daly [1986]). Protracted post-collision tectono-thermal events within the DGC included, *inter alia*, episodic granite emplacements, metamorphism and structural deformation.

The DGC belt is overlain by very thick sedimentary cover, particularly in north-western Botswana. Airborne magnetic and gravity patterns have been used as first-pass tools to map its spatial extent.

The Congo craton comprises several Archean shields and cratons, the southern part made up of the Angolan shield, which consists of granite-gneisses and metasediments, overlain by Paleoproterozoic cover (Begg *et al.* [2009]). The thick sedimentary cover makes the southern Congo craton one of the least understood areas in the African tectonic landscape. The Kalahari craton which includes the Archean Kaapvaal and Zimbabwe cratons separated by high grade Limpopo belt in addition to the Paleoproterozoic crustal components (Rehoboth, Okwa and Magondi terranes) surrounded by late Neoproterozoic/early

Paleozoic mobile belts.

In total, 22 broadband MT stations were deployed in north-western Botswana as part of the regional SAMTEX project (Figure 1). The site spacing was approx. 20 km.

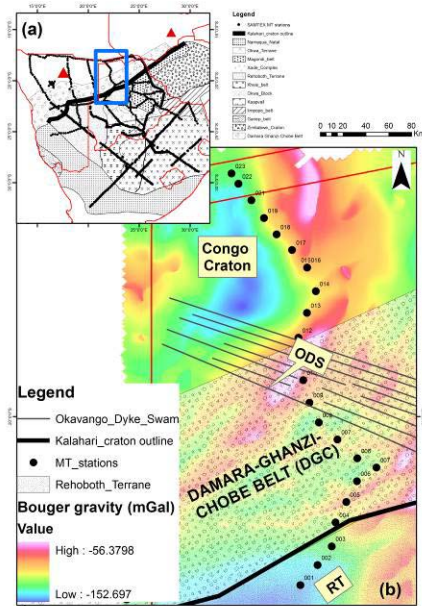


Figure 1. Location of the SAMTEX MT sites (black dots) overlain on the regional tectonic map of southern Africa. The two S-wave receiver functions stations (TSUM and LSZ) are shown as red triangles. (b) Detailed map of the insert in (a) showing the study area and the MT stations (black filled circles) used overlain on the gravity map (rgb scale) of Botswana.

MT DATA AND ANALYSIS

In order to derive the optimum MT impedance responses as a function of period, the measured electric and magnetic field time series were processed and compared using different robust processing codes of *Egbert and Booker [1986]* and the heuristic approach of *Jones et al. [1989]*, the latter implemented in the *Phoenix* processing package *SSMT2000*. Figure 2 shows examples of MT responses from the two sites on the profile, showing apparent resistivity and phase responses for the Transverse Electric (TM/XY) and Transverse Magnetic (TM/YX) modes plotted against increasing period.

MT data decomposition is a critical step in the interpretation process since from it we derive the geo-electric strike and dimensionality parameters which influence/determine our modelling strategy.

In order to remove galvanic distortion from the measured data, to derive the best 2D responses and

obtain the most consistent 2D strike direction, the Groom-Bailey (GB) decomposition technique (*Groom and Bailey [1989]*), which is extended and implemented in the *STRIKE* code of *McNeice and Jones [2001]* was used for each MT site.

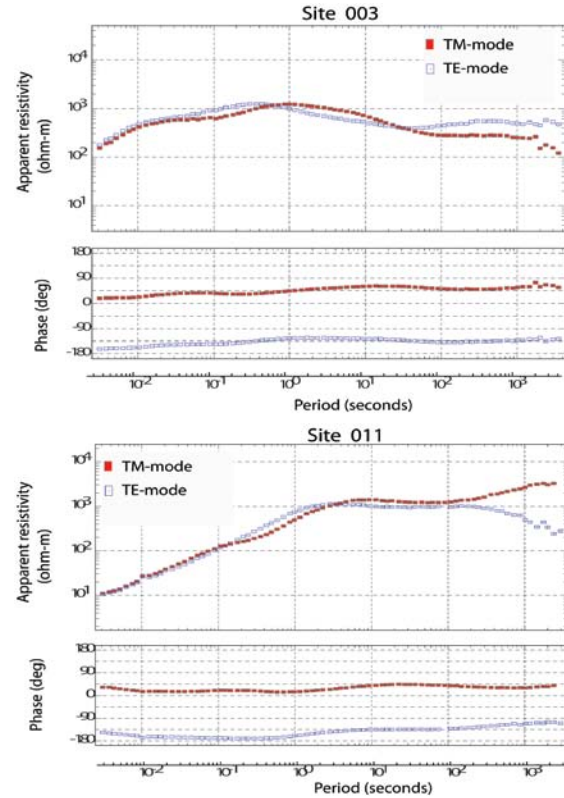


Figure 2. Examples of MT site responses from two sites along the profile. The apparent resistivity and phase for the two polarization modes, TE (XY) and TM (YX) are plotted as a function of increasing period. Site 003 is an example of a 1D MT response, with almost coincident apparent resistivity and phase curves

Since the subsurface structure can exhibit variable degree of dimensionality and directionality, data decomposition was performed for various period (i.e. depth) bands.

Figure 3 shows the results of the single site multi-period decomposition determined for crustal and mantle depths. Niblett-Bostick depth transformation was applied to obtain maximum depth of penetration estimates for each site.

The large phase difference, indicated by large vector lengths, between the TE and the TM modes infer a strongly 2D electrical structure. The direction of the vector corresponds to the derived strike azimuth for each site. The squared blocks, colour coded by the root-mean-square (RMS) error between the MT response of the 2D GB decomposition model and the observed MT responses. Most of the sites displayed acceptable 2D behaviour (low RMS) and only few sites

exhibit 3D characteristics, particularly within the DGC, which implies a heterogeneous lithosphere.

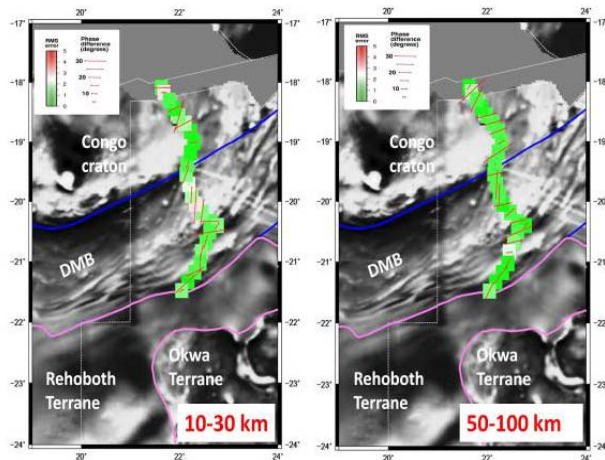


Figure 3. Results of MT data decomposition for crustal (10-30 km) and mantle (50-100 km) depths superimposed on the regional magnetic map of southern Africa

Those sites showing severe 3D and static shift characteristics were not included in the inversion process.

Although site-to-site strike variation is evident, in general there appears to be little depth variation in the geo-electric strike azimuths, with an average strike direction of N50°E found to be a reasonable compromise. This is consistent with the dominant tectonic fabric inferred from the magnetic and geological trends. The MT data for the two profiles were fit with a distortion model in this direction for further modelling.

2D INVERSION RESULTS

The decomposed data were imported into Geosystem's Winglink 2D inversion package that uses a non-linear conjugate gradient (NLG) scheme to search for the smoothest best fit model (Rodi and Mackie [2001]). Several inversion parameters were tested in order to obtain a robust and geologically acceptable model.

A tau value of 5 was used for the two models, after a rigorous search for the tau parameter that gives the optimum RMS L-curve trade-off between data misfit and model roughness. A 100 ohm-m homogeneous half space was used as a starting model. A systematic inversion approach that was followed included inverting first for TE and TM phase responses, by allocating high error floors to apparent resistivities. After a few iterations the apparent resistivities were included and, where available, the vertical magnetic responses ('tipper') added. The reason behind inverting the phase responses first is that they are generally free

of static shift effects. The alpha and beta factors, which control the horizontal smoothness and vertical regularization weighting, were set to 1 and 0 respectively. The resulting model converged to an average RMS 2.79.

DISCUSSIONS

The 2D inversion results reveal a heterogeneous electrical resistivity structure across the DGC (Figure 4). The upper crust of the DGC is characterised by conductive and resistive structures, the latter interpreted to be granitic intrusions related to the Pan-African magmatic events. Geological exposures suggest the presence of magnetite and graphite which could explain the presence of conductive anomalies in the DGC upper crust. It is plausible that during periods of crustal extension and thinning, graphite was preferentially emplacement along grain boundaries, and deep shear movement facilitated graphite inter-connectivity. This strain-induced graphite concentration model would explain the spatial extent of the observed conductivity anomalies. It is thus possible that the 'conductive belt', also suggested by magneto-variation studies of *de Beer et al.* [1982], was formed during the high angle transpressive collision between the Kalahari and Congo cratons.

The stacked S-wave receiver function (SRFs), overlain on the electrical resistivity model, suggests Moho depths of approximately 40 km. Unlike the Moho, the DGC's LAB signal from the SRFs is close to the bootstrap error limits as such this depth is not well resolved. However, the electrical resistivity results suggest the LAB beneath the DGC at approximately 150 km (estimated at 142 km from SRFs).

Evident on the resistivity model is the resistive (i.e. colder), thicker lithosphere north of the DGC, related to the southern edge of the Congo craton. The LAB beneath the Congo craton at the Namibia/Angola border is inferred to be at depths of approx 240 km. It should be noted that subsurface Pre-Cambrian geology maps (*Singletary et al.* [2003]) suggest that the boundary drawn based on the distinct magnetic pattern corresponds to the Neoproterozoic Ghanzi Group of rocks within the Ghanzi-Chobe belt and *not* the tectonic margin between the intra-cratonic DGC orogen and the Congo craton.

The Okavango Dyke Swam (ODS), with an approximate width of 100 km, appears as a very resistive (10000 Ωm) crustal feature extending to depths of 50 km. The dykes are mainly doleritic in composition and are hosted by granite gneisses, which would account for the high resistivities. The Rehoboth Terrane, which forms the part of the northern Kalahari craton, has a relatively thicker lithosphere (>160 km).

CONCLUSIONS

Based on our electrical resistivity models and the known outcropping geology, it is inferred that the Kalahari and Congo craton lithosphere extends and significantly thins beneath the Damara-Ghanzi-Chobe orogen. Our results provide the first pseudo three-dimensional electrical resistivity map of the crustal and mantle lithosphere beneath the DGC and its surrounding tectonic blocks, constraining the previously unknown deep geometry of the Kalahari and Congo craton in the region.

ACKNOWLEDGEMENTS

The SAMTEX consortium members (Dublin Institute for Advanced Studies, Woods Hole Oceanographic Institution, Council for Geoscience (South Africa), De Beers Group Services, The University of the Witwatersrand, Geological Survey of Namibia, Geological Survey of Botswana, Rio Tinto Mining and Exploration, BHP Billiton, Council for Scientific and Industrial Research (South Africa) and ABB Sweden) are thanked for their funding and logistical support during the four phases of data acquisition. SAMTEX project is also funded by the Science Foundation Ireland grant number 05/RFP/GEO001. The magnetic data is courtesy of the Council for Geoscience South Africa and the gravity data was kindly supplied by the Geological Survey of Botswana. We are also indebted to many farmers and landowners throughout southern Africa for their unrewarded co-operation in allowing the deployment of MT stations on their properties.

REFERENCES

Begg, G., et al. (2009), The lithospheric architecture of Africa: Seismic tomography, mantle petrology, and tectonic evolution, *Geosphere*, 5(1), 23{50, doi:10.1130/GES00179.1.

Daly, M. C. (1986), Crustal shear zones and thrust belts: their geometry and continuity in central Africa, *Phil. Trans. R. Soc Lond.*, 317(1539), 111{128, doi:10.1098/rsta.1986.0028.

de Beer, J. H., R. M. J. Huysen, S. J. Joubert, and J. S. V. Zijl (1982), Magnetometer array studies and deep Schlumberger soundings in the Damara orogenic belt, south west Africa, *Geophysical Journal of the Royal Astronomical Society*, 70(1), 11{29, doi:10.1111/j.1365-246X.1982.tb06388.x.

Egbert, G. D., and J. R. Booker (1986), Robust estimation of geo magnetic transfer functions, *Geophysical Journal of the Royal Astronomical Society*, 87(1)173{194, doi:10.1111/j.1365-246X.1986.tb04552.x.

Groom, R. W., and R. C. Bailey (1989), Decomposition of magnetotelluric impedance tensors in the presence of local three-dimensional galvanic distortion, *Journal of Geophysical Research*, 94(2), 1913{1925, doi:10.1029/JB094iB02p01913.

Hansen, S. E., A. A. Nyblade, and J. Julia (2009), Estimates of crustal and lithospheric thickness in Sub-Saharan Africa from S-wave receiver functions, *South African Journal of Geology*, 112(3-4), 229{240, doi:10.2113/gssajg.112.3-4.229.

Jones, A. G., A. Chave, G. Egbert, D. Auld, and K. Bahr (1989), A comparison of techniques for magnetotelluric response function estimation, *Journal of Geophysical Research*, 94(10), 14,201{14,213, doi:10.1029/JB094iB10p14201.

McNeice, G. W., and A. G. Jones (2001), Multisite, multifrequency tensor decomposition of magnetotelluric data, *Geophysics*, 66(1), 158{173, doi:10.1190/1.1444891.

Rodi, W., and R. L. Mackie (2001), Nonlinear conjugate gradients algorithm for 2D magnetotelluric inversion, *Geophysics*, 66, 174{187}

Singleton, S. J., R. E. Hanson, M. W. Martin, J. L. Crowley, S. A. Bowring, R. M. Key, L. V. Ramokate, B. B. Direng, and M. A. Krol (2003), Geochronology of basement rocks in the Kalahari desert, Botswana, and implications for regional Proterozoic tectonics, *Precambrian Research*, 121, 47{71(25), doi:10.1016/S0301-9268(02)0020

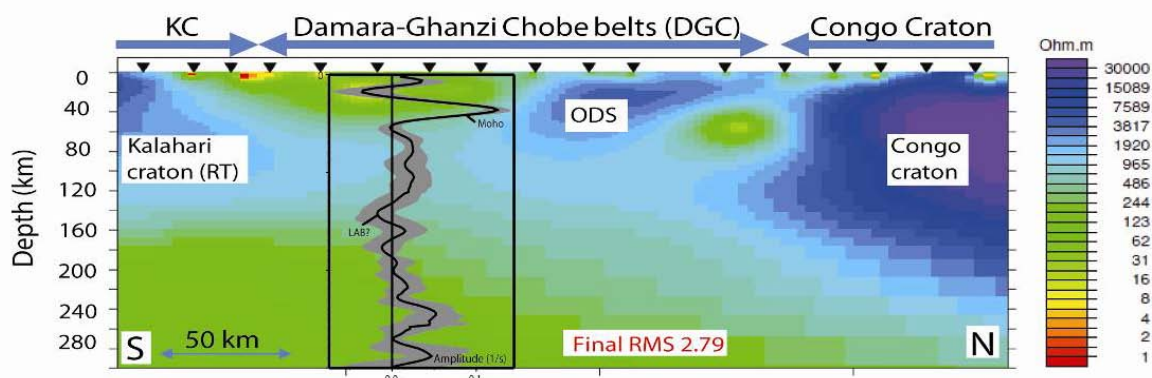


Figure 4. 2D electrical resistivity model derived from smooth inversion of the MT data. The RMS 2.79 respectively. Abbreviations used: ODS=Okavango Dyke Swam, RT=Rehoboth Terraine. The inverted black triangles denote sites locations and the vertical exaggeration is 1.0. Superimposed on the resistivity model is the stacked S-wave receiver function (after Hansen et al. [2009]) located within the Damara belt. The black line shows the mean stack while the grey shaded areas indicate the 2σ bootstrap error bounds. The Moho and LAB phase conversions are indicated.